Sains Malaysiana 51(4)(2022): 1005-1015
http://doi.org/10.17576/jsm-2022-5104-05

Wackestones and Grainstones Geochemistry from Baturaja Formation, South Sumatra Province, Indonesia: Origin and Depositional Environment

(Geokimia Batu Wak dan Batu Butir dari Formasi Baturaja, Wilayah Selatan Sumatera, Indonesia: Asal Usul dan Persekitaran Pengendapan)

RONALDO IRZON[1]*, SIGIT MARYANTO[1], ILDREM SYAFRI[2], KURNIA[1], HERI HERMIANTO JAZULI[1] & PRIYO HARTANTO[3]

[1]*Center for Geological Survey, Jl. Diponegoro 57, Bandung 40122, Indonesia*
[2]*Faculty of Technical Geology, Padjadjaran University, Jalan Raya Bandung-Sumedang Jatinangor, Sumedang 45363, Indonesia*
[3]*Indonesian Institute of Science, Jl. Ganesha No.10, Bandung 40132, Indonesia*

Received: 25 February 2021/Accepted: 15 August 2021

ABSTRACT

Limestone members of the Baturaja Formation at Rambangnia Traverse in Sumatra are classified into wackestones, packstones, grainstones, and floatstones based on microfacies discrimination. This study compared the geochemistry characteristics of the wackestones and the grainstones at the traverse to define their material origins and sedimentation environment. A total of ten samples were analyzed using XRF for 11 oxides and 12 trace elements composition. The samples are carbonates with a minimum fraction of dolomite or magnesite. Clastic material of eroded Kikim Formation is the major impurity origin in the limestone without considerable sulfate content. The wackstones signify a higher detrital input rate and contain more clay which increased during CaO separation than the grainstones. Iron in the wackstones was lost through diagenesis while sodium in the grainstones was precipitated directly from seawater. According to V/Cr and Cu/Zn ratios, the wackestones were deposited in more oxic condition than the grainstones. The studied carbonates have not been affected by a considerable post-depositional alteration based on their geochemistry characteristics.

Keywords: Baturaja Formation; geochemistry; grainstones; limestone; wackestones

ABSTRAK

Ahli batu kapur Formasi Baturaja di rentas Rambangnia di Sumatera dikelaskan kepada batu wak, batu padat, batu butir dan batu terapung berdasarkan diskriminasi mikrofasies. Kajian ini membandingkan ciri-ciri geokimia batu wak dan batu butir pada rentas untuk menentukan asal bahan dan persekitaran pemendapan. Sebanyak sepuluh sampel telah dianalisis menggunakan XRF untuk 11 oksida dan 12 komposisi unsur surih. Sampel adalah karbonat dengan pecahan minimum dolomit atau magnesit. Bahan klastik Formasi Kikim yang terhakis adalah asal kekotoran utama dalam batu kapur tanpa kandungan sulfat yang banyak. Batu wak menandakan kadar input detrital yang lebih tinggi dan mengandungi lebih banyak tanah liat yang meningkat semasa pemisahan CaO daripada batu butir. Besi dalam batu wak telah hilang melalui diagenesis manakala natrium dalam batu kikir daripada air laut secara terus. Menurut nisbah V/Cr dan Cu/Zn, batu wak telah dimendapkan dalam keadaan oksik yang lebih banyak daripada batu butir. Karbonat yang dikaji tidak terjejas oleh perubahan pasca pemendapan yang besar berdasarkan ciri geokimia mereka.

Kata kunci: Batu butir; batu kapur; batu wak; geokimia; Formasi Baturaja

INTRODUCTION

Geochemistry is an essential tool in the earth science investigations. Geochemistry characters of sedimentary rocks are useful in interpreting the depositional environment, material origin, diagenesis, and tectonic setting (Adenan et al. 2017; Al-Dabbas et al. 2014; Coimbra & Olóriz 2012; Elmagd et al. 2018; Hood et al. 2018; Irzon & Maryanto 2016; Zhang et al. 2017).

Both mineral and contaminant sources were traced using geochemical compositions of stream sediments (Phewnil et al. 2012; Yousefi et al. 2012). Integrated petrography and geochemistry should bring out precise and accurate conclusions.

Limestones, constituting approximately ~15% of the continental surface, is the main portion of the Earth's sedimentary shell. The carbonate rocks are mainly built of calcium carbonate and highly influenced by climatic and environmental conditions (Zhang et al. 2017). Metalliferous and terrigenous particulates and scavenging from seawater lead to a variety of chemical contents in limestones. The dead organisms, including corals and planktons, contains in shelly limestones are essential for relative dating of the Earth's evolution (Asis & Jasin 2015; Okuyucu et al. 2013). Microfacies variation in limestones can help in the diagenesis interpretations including cementation, lithification, solution, and alteration process of the sediments (El-Sorogy et al. 2016; Hussain et al. 2013; Maryanto 2014). Correlations of oxides and elements can determine limestones' diagenesis, the source of terrigenous materials, and sedimentation properties (Al-Dabbas et al. 2014; Babu et al. 2014; Elmagd et al. 2018; Ganai et al. 2018; Usman et al. 2018). Instead of being classified as heavy metal pollution (Kabir et al. 2020), chromium and zinc compositions are also essential in limestones depositional studies. The paleo-redox state during limestone deposition can be assessed by geochemical ratios such as V/Cr, V/(V + Ni), U/Th, and Cu/Zn (Abedini et al. 2020; Mir 2015; Palomares et al. 2012) while postsedimentation transformation of carbonates can be determined by Mg/Ca, Fe/Sr, and Mn/Sr ratios (Romero et al. 2013; Vishnevskaya et al. 2012).

Limestones from several formations are widespread in Sumatra and were formed since the Paleozoic to Miocene time. The carbonate members of the Baturaja Formation which were deposited during the Early Miocene in a back-reef environment are exposed near Muaradua, South Sumatra, with a total thickness of 120 m (Maryanto 2007). According to a detailed microfacies and petrographic analysis along the Rambangnia Traverse, the carbonate rocks consist of wackestone, packstone, grainstone, and floatstone (Maryanto 2014). In general, these facies occurred repeatedly and developed in a transgressive depositional neighbourhood. Moreover, the depositional environment varies from the restricted bay, back-reef, slope, shelf edge, winnowed platform, and reef-flank. A geochemical investigation of the limestone is required to identify the diagenesis, detrital factor, and sedimentation properties of the rock. The purpose of this study is to compare the geochemical characteristics of the wackestones and the grainstones at the Rambangnia Traverse to predict their material origins and sedimentation environment.

Materials and Methods

General Geology

The studied location is part of the Geological Map of Baturaja Quadrangle, Sumatra (Gafoer et al. 1993) which consists of Pre-Tertiary to Quaternary rock units (Figure 1). The Pre Tertiary rocks or formations include Tarap Formation, Garba granite, Garba Formation and Melange complex. Kikim Formation and Talangakar Formation were built in the Paleogene while Baturaja Formation, Gumai Formation, Airbenakat Formation, and Muaraenim Formation during the Miocene. The studied limestone samples are from the Baturaja Formation in the Muaradua Regency, South Sumatra. Ranau Formation, Kasai Formation, a couple of volcanic units, and Alluvium were emplaced in the Quarternary.

Limestone members of the Baturaja Formation were generally deposited in the back-reef environment behind the edge of the South Sumatra Basin (Aswan et al. 2017; Maryanto 2007). Layered limestones can be observed directly along the studied area, the Air Rambangnia traverse. The carbonate rocks are generally dipping to the east with a total thickness reaching 220 m. The thickness of the Baturaja Formation is up to 196 m. The Baturaja Formation limestone unconformably overlies the volcanic Kikim Formation. The lower part of the Baturaja Formation is marked by the presence of grainstone containing porosity. Furthermore, the layered and mud-supported wackestone and packstone were developed above it. Some part of Gumai Formation is also built of limestone and is located close to the Baturaja Formation (Gafoer et al. 1993). Even though both limestones from Baturaja Formation and Gumai Formation were formed during the Early to Middle Miocene, they were deposited in different redox states with unequal terrigenous input according to their geochemical characteristics (Irzon & Maryanto 2016).

Sample Description

The studied samples comprised of seven wackestones and three grainstones from the Baturaja Formation in

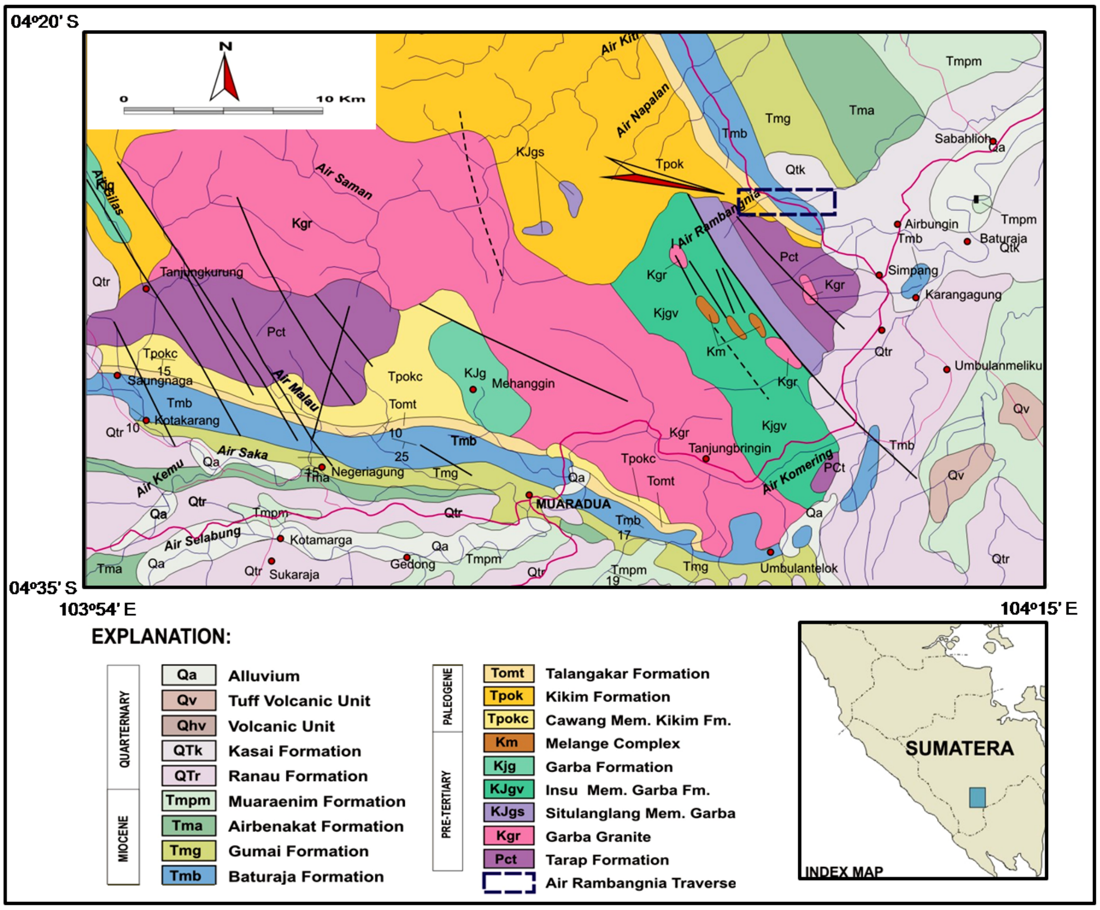

FIGURE 1. Rambangnia Traverse located in the domain of Baturaja Formation (Tmb) at the South Sumatra Province (Gafoer et al. 1993)

Rambangnia Traverse. The wackestones consist of SM 304A, SM 305A, SM 305B, SM 314A, SM 315A, SM 321A, and 323C while SM 324A, SM 324B, and SM 324C are the grainstones. Although all the selected samples show bioclastic fragmented, the grainstones are moderately sorted with open fabric whilst the wackestones are poor-very poorly sorted with close fabric. Lithostratigraphically, the grainstones were deposited above the wackestones (Figure 2).

ANALYTICAL PROCEDURES

The limestones were delivered to the Laboratory of Center for Geological Survey Indonesia in Bandung for preparation and geochemical content measurement using XRF. Before crushing and milling to gain the < 200 mesh fraction, the carbonates were dried outdoor under sunlight for at least one day. Flexibility and accuracy are the main reason for using the pressed pellet method other than the fused bead for XRF analysis (Bamrah et al. 2019; Irzon et al. 2020). Pellet thickness should be more than the stainless steel ring in avoiding incorrect detection of X-ray radiation (Irzon et al. 2020). Eleven oxides (SiO_2, TiO_2, Al_2O_3, Fe_2O_{3T}, MnO, CaO, MgO, Na_2O, K_2O, P_2O_5, and SO_3) and twelve trace elements (Zn, Zr, Hg, Cs, Cu, Sr, V, Cr, Cl, Rb, Y, and Sc) compositions were analyzed using Advant-XP XRF. LOI was measured by adopting the previous method of Irzon (2018) and Irzon et al. (2021) through heating the sample to 1000 °C. The geochemistry composition of the samples is shown in Table 1.

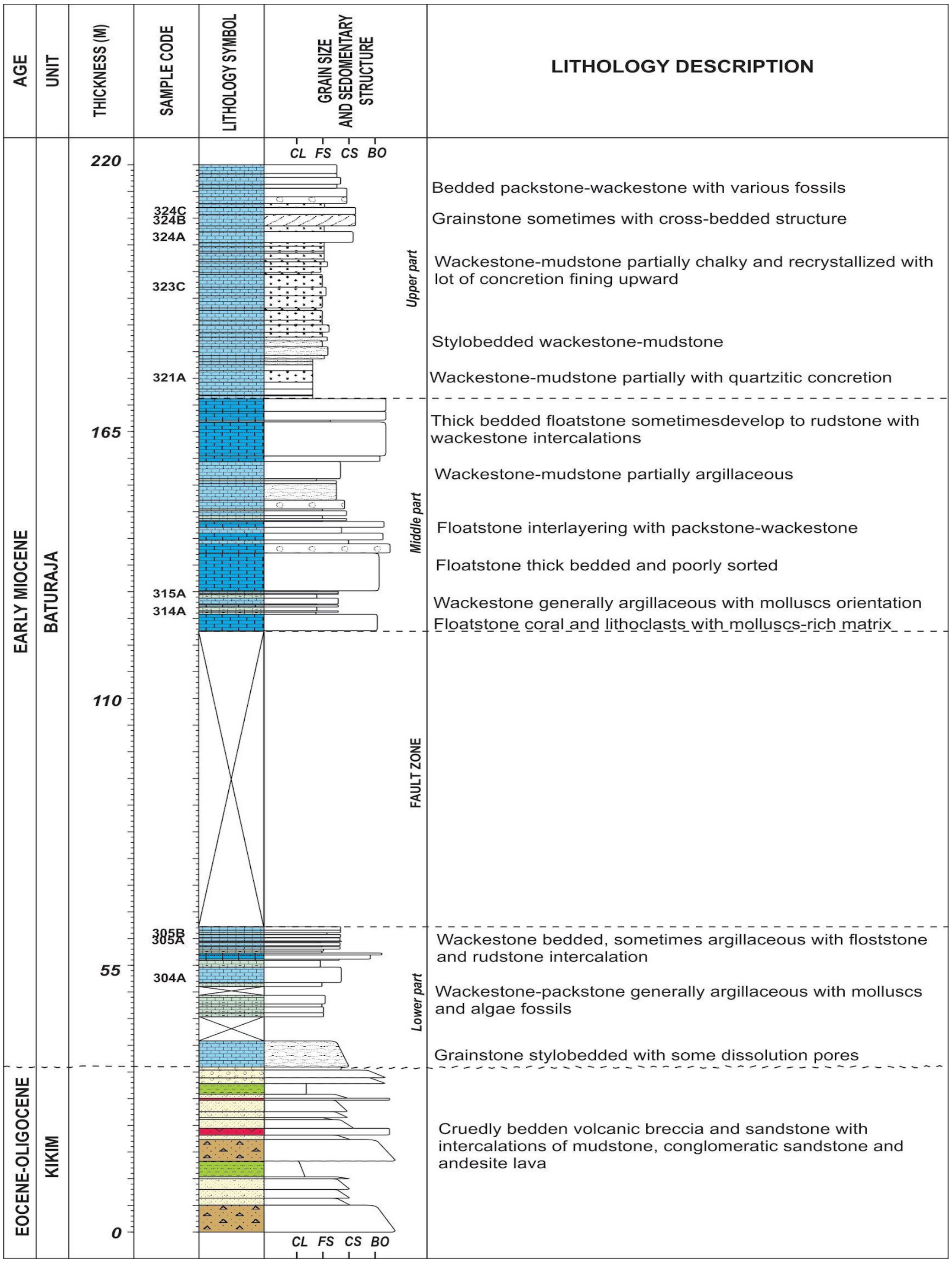

FIGURE 2. The studied samples in a detailed lithostratigraphy column along Air Rambangnia traverse, South Sumatra (modified after Maryanto 2014). Grain size: CL = clay, FS = fine sand, CS = coarse sand, BO = boulders

TABLE 1. Chemical compositions of the slimestone samples from Baturaja Formation

	Wackestones							Grainstones		
Sample Code	SM 304A	SM 305A	SM 305B	SM 314A	SM 315A	SM 321A	SM 323C	SM 324A	SM 324B	SM 324C
Major oxides (%)										
SiO_2	7.97	6.85	6.74	6.33	7.97	7.97	7.89	3.54	4.35	3.88
TiO_2	0.15	0.05	0.05	0.07	0.22	0.14	0.15	0.03	0.02	0.04
Al_2O_3	3.50	2.44	2.00	2.35	2.87	3.49	3.26	2.05	2.13	2.00
Fe_2O_{3T}	2.02	1.70	1.42	2.02	2.28	2.02	1.85	1.24	1.23	1.39
MnO	0.25	0.13	0.16	0.25	0.19	0.15	0.23	0.13	0.14	0.16
CaO	45.61	49.19	48.62	45.72	46.48	44.81	45.27	50.12	50.25	50.68
MgO	0.85	0.60	0.83	0.76	0.87	0.85	0.64	0.37	0.43	0.38
Na_2O	0.02	0.04	0.03	0.03	0.01	0.01	0.02	0.07	0.08	0.06
K_2O	0.08	0.05	0.03	0.06	0.08	0.08	0.08	0.10	0.10	0.09
P_2O_5	0.05	0.08	0.03	0.05	0.06	0.05	0.05	0.03	0.03	0.02
SO_3	0.16	0.17	0.12	0.08	0.03	0.15	0.16	0.05	0.05	0.06
LOI	39.01	38.64	40.52	41.20	38.93	40.76	40.11	41.32	41.04	40.84
Trace elements (ppm)										
Zn	162	84	124	90	80	123	66	55	60	36
Zr	54	36	44	35	64	75	48	24	29	31
Hg	24	18	22	16	27	24	31	43	57	51
Cs	85	75	68	77	54	66	86	84	86	77
Cu	95	56	102	88	77	84	80	64	58	59
Sr	346	432	328	410	267	364	336	653	665	587
V	74	65	68	77	58	62	47	106	152	123
Cr	46	65	62	48	52	46	22	24	26	18
Cl	143	214	166	147	168	174	225	285	361	322
Rb	95	102	98	88	110	104	86	26	38	42
Y	346	366	324	402	348	335	375	485	479	475
Sc	74	88	58	96	75	69	83	192	122	106

Results and Discussion

The limestone samples show high CaO content of between 44.81-49.19% and 50.12-50.68% for wackestones and grainstones, respectively. The SiO_2, Al_2O_3, and Fe_2O_3 compositions of the wackestones are higher than the grainstones but with less organic matter and carbonate contents based on the LOI comparison. Seven other oxides are counted minors with the abundances < 1%. Overall, the samples of this geochemical data set are narrowed within < 16 wt.% for their non-CaO–LOI content. Sr is the most abundant trace element with an average > 500 ppm. Yttrium and chlorine average > 200 ppm while the other measured trace elements < 100 ppm. The wackstones contain more Zn, Zr, Cu, Cr, and Rb but less Hg, Cs, Sr, V, Cl, Y, and Sc than the grainstones. Correlation coefficients of the oxides and associated elements are shown in Table 2.

TABLE 2. Correlation coefficient values of oxides and elements in the studied samples

a) The Wackestones

	SiO_2	TiO_2	Al_2O_3	Fe_2O_{3T}	MnO	CaO	MgO	Na_2O	K_2O	P_2O_5	LOI	Zn	Zr	Cu	Sr	V	Cr	Rb	Y
TiO_2	0.89	1.00																	
Al_2O_3	0.77	0.70	1.00																
Fe_2O_{3T}	0.53	0.78	0.72	1.00															
MnO	-0.16	-0.12	0.02	-0.10	1.00														
CaO	-0.57	-0.65	-0.78	-0.71	-0.38	1.00													
MgO	0.32	0.44	0.02	0.37	-0.02	-0.28	1.00												
Na_2O	-0.83	-0.80	0.60	-0.48	0.15	0.60	-0.70	1.00											
K_2O	0.85	0.89	0.94	0.83	0.00	-0.84	0.22	-0.67	1.00										
P_2O_5	0.12	0.08	0.50	0.35	-0.46	0.01	-0.57	0.29	0.32	1.00									
LOI	-0.36	-0.29	-0.23	-0.16	0.43	-0.34	0.15	-0.08	-0.19	-0.56	1.00								
Zn	0.38	0.10	0.12	-0.14	0.08	0.00	0.54	-0.41	0.06	-0.32	-0.20	1.00							
Zr	0.81	0.75	0.56	0.52	-0.37	-0.54	0.64	-0.95	0.68	-0.07	-0.02	0.41	1.00						
Cu	-0.01	0.02	-0.25	-0.14	0.62	0.23	0.67	-0.36	-0.12	-0.93	0.53	0.49	0.14	1.00					
Sr	-0.61	-0.74	-0.07	-0.31	0.11	0.19	-0.63	0.73	-0.37	0.45	0.17	-0.18	-0.57	-0.38	1.00				
V	-0.55	-0.48	-0.48	-0.06	0.29	0.17	0.30	0.37	-0.40	-0.17	0.16	0.33	-0.33	0.36	0.43	1.00			
Cr	-0.51	-0.53	-0.61	-0.34	-0.52	0.78	0.15	0.38	-0.67	0.05	-0.26	0.22	-0.22	-0.13	0.23	0.56	1.00		
Rb	0.30	0.30	0.00	0.24	-0.89	0.28	0.44	-0.38	0.09	0.22	-0.47	0.25	0.56	-0.29	-0.35	-0.07	0.58	1.00	
Y	-0.41	-0.17	0.14	0.25	0.38	-0.24	-0.57	0.57	0.07	0.41	0.19	-0.75	-0.58	-0.34	0.51	0.09	-0.33	-0.61	1.00
Sc	-0.34	-0.15	0.25	0.33	0.18	-0.18	-0.62	0.59	0.13	0.65	-0.02	-0.70	-0.52	-0.55	0.59	0.10	-0.21	-0.43	0.96

b) The Grainstones

	SiO_2	TiO_2	Al_2O_3	Fe_2O_{3T}	MnO	CaO	MgO	Na_2O	K_2O	P_2O_5	LOI	Zn	Zr	Cu	Sr	V	Cr	Rb	Y
TiO_2	-0.71	1.00																	
Al_2O_3	0.70	0.12	1.00																
Fe_2O_{3T}	-0.18	0.91	-0.29	1.00															
MnO	0.35	0.57	-0.75	0.85	1.00														
CaO	-0.65	0.75	-0.57	0.95	0.97	1.00													
MgO	0.99	-0.67	-0.81	-0.32	0.22	0.10	1.00												
Na_2O	0.43	-0.99	0.04	-0.97	-0.69	-0.85	0.31	1.00											
K_2O	0.20	-0.92	0.28	-1.00	-0.84	-0.74	-0.32	0.75	1.00										
P_2O_5	-0.36	-0.56	0.76	-0.85	-1.00	-0.53	-0.67	0.41	0.91	1.00									
LOI	-0.48	-0.45	0.83	-0.77	-0.99	-0.76	0.04	0.46	0.13	-0.04	1.00								
Zn	0.60	-1.00	-0.15	-0.90	-0.54	-0.71	0.52	0.97	0.61	0.22	0.37	1.00							
Zr	0.62	0.30	-0.91	0.66	0.95	0.67	0.75	-0.40	-0.85	-0.95	-0.24	-0.18	1.00						
Cu	-0.89	0.13	1.00	-0.28	-0.74	-0.15	0.24	-0.12	-0.55	-0.63	0.75	-0.10	0.35	1.00					
Sr	0.24	-0.94	0.24	-1.00	-0.82	-0.71	0.58	0.75	0.18	-0.19	0.79	0.79	0.05	0.54	1.00				
V	1.00	-0.61	-0.86	-0.23	0.31	-0.09	-0.06	0.41	0.70	0.65	-0.58	0.39	-0.38	-0.95	-0.26	1.00			
Cr	0.34	-0.97	0.14	-0.99	-0.76	-0.35	0.74	0.41	-0.27	-0.60	0.69	0.52	0.45	0.75	0.90	-0.54	1.00		
Rb	0.65	0.26	-0.93	0.63	0.94	0.49	0.76	-0.31	-0.85	-0.99	0.02	-0.10	0.96	0.58	0.26	-0.57	0.64	1.00	
Y	0.94	-0.82	-0.67	-0.52	0.00	-0.26	-0.16	0.51	0.82	0.77	-0.43	0.46	-0.54	-0.91	-0.18	0.98	-0.52	-0.69	1.00
Sc	-0.70	-0.20	0.95	-0.58	-0.92	-0.62	-0.79	0.33	0.82	0.94	0.21	0.11	-1.00	-0.36	-0.11	0.37	-0.50	-0.97	0.72

Both groups show the limestone composition according to the CaO-SiO_2-MgO ternary diagram without considerable dolomite or magnesite fraction as shown in Figure 3(a) (Elmagd et al. 2018). High purity of the carbonates and very low Fe-Mg enrichment is shown on Al_2O_3-CaO-(Fe_2O_{3T}+MgO) scheme (Figure 3(b)). However, the grainstones contains less quartz and clay minerals than the wackestones with the average non-CaO–LOI concentration of 8.86 and 13.54 wt.%, respectively. The impurities in the studied samples are generally of clastic origin as confirmed in Figure 3(c) with relatively insignificant sulfate composition. Groupings of both wackestones and grainstones are easily detected in those three triangular diagrams.

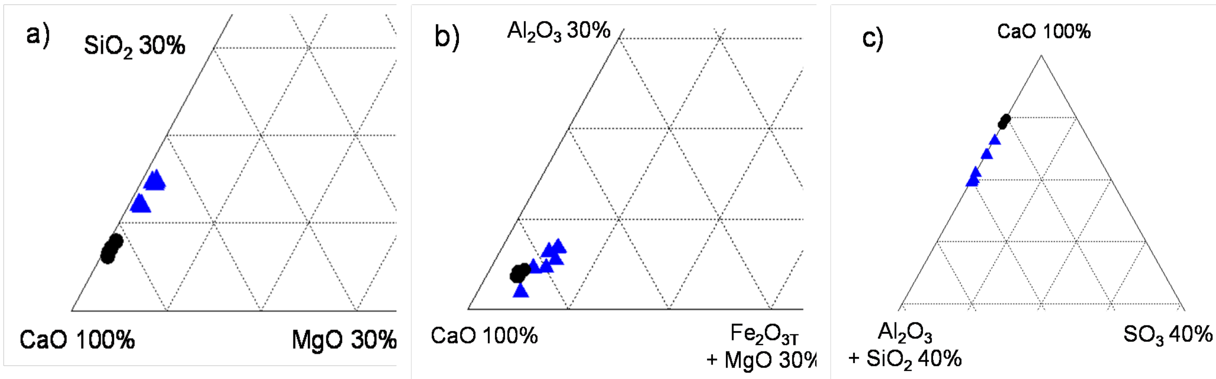

FIGURE 3. Ternary diagrams which portray the purity of the studied rocks. a) the CaO-SiO_2-MgO diagram; b) CaO-Al_2O_3-(Fe_2O_{3T}+MgO) diagram; and c) Al_2O_3+(SiO_2)-CaO-SO_3 diagram

MATERIAL ORIGIN BASED GEOCHEMICAL CHARACTERISTICS

SiO_2 and CaO relationships to other elements are notable in limestones' studies to define the material source of the rock. In the grainstones, TiO_2, Fe_2O_{3T}, MnO, and Zr show strong to moderate positive correlations with CaO whilst SiO_2, Al_2O_3, Na_2O, K_2O, Zn, Sr, and Sc depict negative ones. Na_2O and Cr concentrations of the wackestones increase but SiO_2, TiO_2, Al_2O_3, Fe_2O_{3T}, K_2O, and Zr decrease with the increase of CaO. SiO_2 abundance of the wackestones correlates positively with TiO_2, Al_2O_3, Fe_2O_{3T}, K_2O, Zr, and Hg but negatively with CaO, Na_2O, Sr, and V. TiO_2, CaO, and Cu, and Sc concentrations of the grainstones denote an inverse relationship with SiO_2. On the other hand, the SiO_2 content of this group exhibits positive correlations to Al_2O_3, MgO, Zn, Zr, Hg, V, Rb, and Y.

Reducing SiO_2 content through CaO enrichment in both microfacies groups is normal during carbonates formation. Much higher SiO_2 concentration of the wackestones (7.39% on average) implies a higher detrital material rate than the grainstones (averagely 3.92%) during deposition as shown in Figure 4(a). Volcanic breccia, lava, and sandstone built the Paleocene-Oligocene Kikim Formation at the southeast region of the studied Baturaja Formation. The eroded pieces from the Kikim Formation might be the detrital SiO_2 source of the studied samples. TiO_2, Al_2O_3, Fe_2O_{3T}, K_2O, Zr, and Hg were incorporated in the wacktones formation during the rapid detrital input according to their positive relationship to SiO_2 (Table 2). At a slower pace, quartz associated terrigenous influx brought in MgO, Zn, Zr, Hg, V, Rb, and Y enriched material through grainstones sedimentation.

The Al_2O_3 content in limestones is another indicator of detrital material representing the number of clay minerals and is regarded as a proxy for shale contamination (Abedini & Calagari 2015; Al-Dabbas et al. 2014; Elmagd et al. 2018; Ganai et al. 2018). Alumina concentration in both wackestones and grainstones is in the range from 1 to 3.5 wt.% and higher than the predicted siliciclastic-contaminated carbonates (1.59%) (Veizer 1983) to show a substantial contribution of terrigenous material. Clay minerals in the two microfacies should be derived from detrital input due to the Al_2O_3-SiO_2 positive relationships (Table 2). The clay minerals might be originated from claystone and shale (Abedini & Calagari, 2015; Al-Dabbas et al. 2014). Positive correlation of Sc with Al further implies terrigenous contamination in the carbonates. The wackestones are

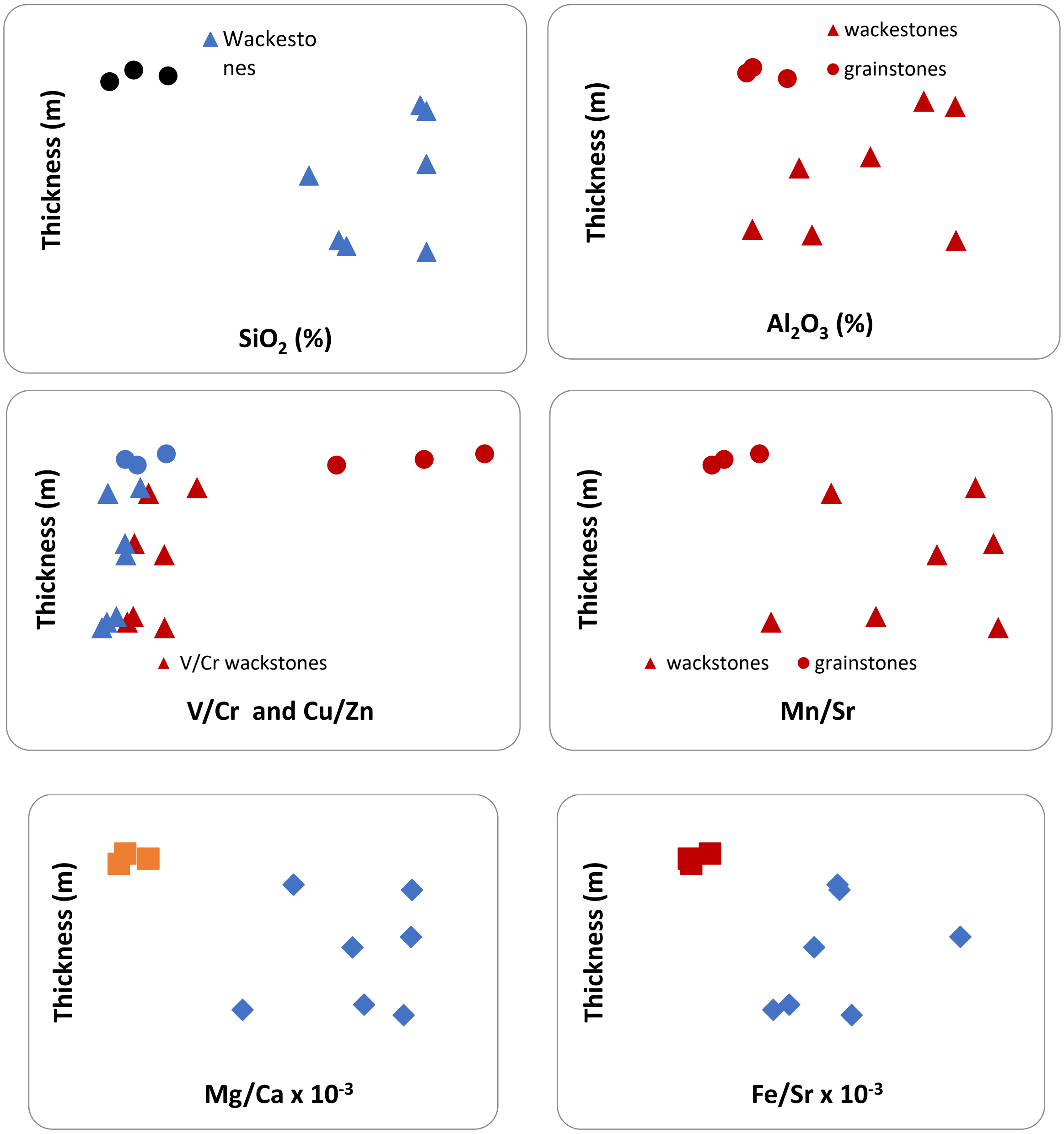

FIGURE 4. Composition and ratios comparison of the wackestones with the grainstones against the thickness.: a)SiO_2 (%); b)Al_2O_3 (%); c) V/Cr and Cu/Zn; d) Mn/Sr; e) Mg/Ca; and f) Fe/Sr

relatively more clayey than the grainstones according to the higher average Al_2O_3 concentration of 2.70 and 2.07%, respectively (Figure 4(b)). Both groups depict a moderate-strong negative CaO-Al_2O_3 correlation to appoint that the clayey materials increased during CaO separation from the limestone solution. The correlation also demonstrates that Ca is not notably influenced by detrital input (e.g. feldspars). Strong positive relationship of Al_2O_3-K_2O ($r = 0.94$) and SiO_2-K_2O ($r = 0.85$) suggest the presence of K-feldspar as a terrigenous fraction of the studied wackestones.

Early limestones are the conversion of dissolved calcium and carbon dioxide as $CaCO_3$ as a result of biochemical activity. Therefore, the relationships of elements with CaO suggest the diagenesis process. MgO of the wackestone correlate negatively to CaO implying that MgO enrichment also because of gradual CaO removal during diagenesis. The very strong negative correlation of Fe_2O_{3T} with CaO of wackstones depicts the loss of iron through diagenesis. The inverse relationship of K_2O with CaO in both groups strengthens the previous description of potassium detrital origin. The positive Na_2O-CaO and negative Na_2O-SiO_2 correlations of wackestones imply direct sodium precipitation from seawater. On the other hand, Na_2O in the grainstones should come from detrital input due to its relationships with SiO_2 and CaO.

A couple of ferromagnesian trace elements, namely, Zr and Cu of the wackestones decrease with the rise of CaO composition because of their input from siliciclastic sediments and parallel with their correlation with SiO_2. The calcitic/aragonitic Ca^{2+} of the wackestones should have been replaced by divalent cations of Zr and Cu. The wackestones' positive Cr correlation with CaO and negative relationship with SiO_2 suggest seawater origin. For grainstones, Zr might enrich from both seawater and siliciclastic sediments. Although no lanthanides were analyzed, the measurement results record the Sc-Y compositions which also classified in the rare earth elements. The strong positive correlation of Sc with Y in both facies emphasized that the REEs were often found together (Irzon 2017; Ma et al. 2019). These two elements increase with the raise of P_2O_5 in both microfacies groups as an indication of the phosphate mineral origin.

DEPOSITIONAL ENVIRONMENT AND POST-DEPOSITIONAL ALTERATION

Chromium is commonly clastic components and detrital origin while vanadium is mainly derived from organic matter and deposited during reducing condition. The comparison between the two trace elements is a tool for paleoredox condition of carbonates. V/Cr ratios of < 2, 2–4.25, and > 4.25 are the indication of oxic, dysoxic, and suboxic–anoxic environments, respectively (Jones & Manning 1994; Madhavaraju et al. 2016). The wackestones were most likely deposited in an oxic environment (V/Cr = 1.42 on average) whilst the grainstones in dysoxic one (V/Cr = 4.06 on average) as shown in Figure 4(c). Reducing depositional condition is represented by high Cu/Zn ratio, whereas low Cu/Zn values signify oxidizing conditions (Mir 2015). Cu/Zn ratios of the studied carbonates are in the range of 0.58 to 1.63 to imply an oxidizing deposition environment. In comparison, the grainstones were deposited in a slightly more reducing environment than the wackstones due to the averagely higher Cu/Zn ratio (Figure 4(c)). Both V/Cr and Cu/Zn ratios indicate a more oxic environment during the wackstones deposition than the grainstones.

The Mn/Sr ratio is a tool to discriminate between the altered and the least altered limestones. After limestone sedimentation, Mn may behave more conservatively, whereas Sr is preferentially leached out because of the exchange with late fluids, leading to a rise of the Mn/Sr ratio (Ganai et al. 2018; Hood et al. 2018). The Mn/Sr ratios in the studied limestones (Figure 4(d)) are generally decreasing from wackstones (3.43 on average) to grainstones (1.75 on average), with variable Sr and Mn contents from 267 to 665 ppm and from 1000 to 1900 ppm, respectively. The studied limestones can be considered as well-preserved carbonates which have not been affected by a considerable post-depositional alteration with Mn/Sr < 5 (Hood et al. 2018). However, the wackestones show a higher degree of alteration than the grainstones.

Postsedimentation transformation of carbonates is also evidenced by Mg/Ca and Fe/Sr ratios (Devi & Duarah 2015; Romero et al. 2013; Vishnevskaya et al. 2012). Adapting the standard Mg/Ca ratio of Todd (1966), the studied carbonates are classified as pure limestone. The average Fe/Sr of wackestones and grainstones is 4.21 and 1.75, respectively, to suggest that the rock experienced a minimum degree of alteration (Kutnetzov et al. 2008). Wackestones have been relatively more affected by diagenesis than grainstones according to the higher Mg/Ca and Fe/Sr ratios and strengthen the previous discussion about Mn/Sr ratio.

CONCLUSION

A total of ten limestones sample which consisted of wackestones and grainstones from Rambangnia Traverse were analyzed. Based on their geochemical characteristics, the rocks contain minimum dolomite or magnesite fraction. Eroded Clastic material is the major source of impurity without substantial sulfate content. Clastic material of eroded Kikim Formation is the major impurity origin in the limestone without considerable sulfate content. Sodium in the grainstones might be seawater origin and added during diagenesis while iron in the wackstones was reduced through the process. Based on V/Cr and Cu/Zn ratios, the wackestones were deposited in more oxic condition than the grainstones. All the samples are limestones with minimum post-depositional alteration. In comparison, the wackestones experienced a more diagenesis effect than the grainstones according to Mn/Sr, Mg/Ca, and Fe/Sr ratios.

ACKNOWLEDGEMENTS

The authors thank Dr. Eko Budi Lelono as the Head of the Center for Geological Survey of Indonesia for data publication. We were financially supported by the Ministry of Energy and Mineral Resources Indonesia. Thanks also go to Mr. Purnama Sendjaja, Mr. Joko Subandrio, and Mr. Verry Edi Setiawan who helped a lot regarding geological interpretation. Mrs. Irfanny Agustiany S.Sc., Ms. Citra Okta Hagia and Ms. Indah Yuni Prasetyawati who assisted us in laboratory works.

REFERENCES

Abedini, A. & Calagari, A.A. 2015. Rare earth element geochemistry of the Upper Permian limestone: The Kanigorgeh mining district, NW Iran. *Turkish Journal of Earth Sciences* 24(4): 365-382.

Abedini, A., Azizi, M.R. & Dill, H.G. 2020. Formation mechanisms of lanthanide tetrad effect in limestones: An example from Arbanos district, NW Iran. *Carbonates and Evaporites* 35(1): 1.

Adenan, N.B., Ali, C.A. & Mohamed, K.R. 2017. Diagenetic history of the Chuping limestone at Bukit Tungku Lembu, Perlis, Malaysia. *Sains Malaysiana* 46(6): 887-895.

Al-Dabbas, M.A., Awadh, S.M. & Zaid, A.A. 2014. Facies analysis and geochemistry of the Euphrates Formation in Central Iraq. *Arabian Journal of Geosciences* 7(5): 1799-1810.

Asis, J. & Jasin, B. 2015. Miocene larger benthic foraminifera from the Kalumpang Formation in Tawau, Sabah. *Sains Malaysiana* 44(10): 1397-1405.

Aswan, Abdurrachman, M., Fitriana, B.S., Mustofa, M.F., Santoso, W.D., Rudyawan, A., Rahayu, W.D., Hamdani, A., Rohiman, Y. & Oo, T.Z. 2017. Paleoenvironmental study of miocene sediments from JTB-1 and NRM-1 wells, in West Ogan Komering block, Meraksa area, South Sumatra Basin. In *IOP Conference Series: Earth and Environmental Science* 71(1): 012033.

Babu, K., Prabhakaran, R., Subramanian, P. & Selvaraj, B. 2014. Geochemical characterization of Garudamangalam limestone cretaceous of Ariyalur Tamilnadu, India. *International Journal of Geology, Agriculture and Environmental Sciences* 2: 17-22.

Bamrah, R.K., Vijayan, P., Karunakaran, C., Muir, D., Hallin, E., Stobbs, J., Goetz, B., Nickerson, M., Tanino, K. & Warkentin, T.D. 2019. Evaluation of x-ray fluorescence spectroscopy as a tool for nutrient analysis of pea seeds. *Crop Science* 59(6): 2689-2700.

Coimbra, R. & Olóriz, F. 2012. Geochemical evidence for sediment provenance in mudstones and fossil-poor wackestones (upper Jurassic, Majorca Island). *Terra Nova* 24(6): 437-445.

Devi, K.R. & Duarah, B.P. 2015. Geochemistry of Ukhrul limestone of Assam-Arakan subduction basin, Manipur, Northeast India. *Journal of the Geological Society of India* 85(3): 367-376.

El-Sorogy, A.S., Almadani, S.A. & Al-Dabbagh, M.E. 2016. Microfacies and diagenesis of the reefal limestone, callovian Tuwaiq mountain limestone formation, central Saudi Arabia. *Journal of African Earth Sciences* 115: 63-70.

Elmagd, A.K., Emam, A., Ali-Bik, M.W. & Hazem, M. 2018. Geochemical assessment of Paleocene limestones of Sinn El-Kaddab Plateau, South Western Desert of Egypt, for industrial uses. *Arabian Journal of Geosciences* 11(13): 355.

Gafoer, S., Amin, T.C. & Pardede, R. 1993. *Geological Map of the Baturaja Quadrangle, Sumatera (1: 250,000).* Indonesia: Geological Research and Development Centre.

Ganai, J.A., Rashid, S.A. & Romshoo, S.A. 2018. Evaluation of terrigenous input, diagenetic alteration and depositional conditions of Lower Carboniferous carbonates of Tethys Himalaya, India. *Solid Earth Sciences* 3(2): 33-49.

Hood, A.S., Planavsky, N.J., Wallace, M.W. & Wang, X. 2018. The effects of diagenesis on geochemical paleoredox proxies in sedimentary carbonates. *Geochimica et Cosmochimica Acta* 232: 265-287.

Hussain, H.S., Fayaz, M., Haneef, M., Hanif, M., Jan, I.U. & Gul, B. 2013. Microfacies and diagenetic-fabric of the Samana Suk Formation at Harnoi Section, Abbottabad, Khyber Pakhtunkhwa, Pakistan. *Journal of Himalayan Earth Science* 46(2): 79-91.

Irzon, R. 2018. Comagmatic andesite and dacite in Mount Ijo, Kulonprogo: A geochemistry perspective. *Jurnal Geologi dan Sumberdaya Mineral* 19(4): 221-231.

Irzon, R. 2017. Geochemistry of late triassic weak peraluminous a-type Karimun granite, Karimun regency, Riau Islands Province. *Indonesian Journal on Geoscience* 4(1): 21-37.

Irzon, R. & Maryanto, S. 2016. Geokimia batugamping Formasi Gumai dan Formasi Baturaja di Wilayah Muaradua, Ogan Komring Ulu Selatan, Wilayah Sumatera Selatan. *Jurnal Geologi dan Sumberdaya Mineral* 17(3): 125-138.

Irzon, R., Syafri, I., Suwarna, N., Hutabarat, J., Sendjaja, P. & Setiawan, V.E. 2021. Geochemistry of granitoids in Central Sumatra: An identification of plate extension during triassic. *Geologica Acta* 19(9): 1-14.

Irzon, R., Kurnia, K. & Haryanto, A.D. 2020. Presisi pengukuran produk samping tambang timah nudur menggunakan analisis XRF dan peluang ekonomi produknya. *Jurnal Teknologi Mineral dan Batubara* 16(2): 69-79.

Jones, B. & Manning, D.A. 1994. Comparison of geochemical indices used for the interpretation of palaeoredox conditions in ancient mudstones. *Chemical Geology* 111(1-4): 111-129.

Kabir, M.H., Islam, M.S., Tusher, T.R., Hoq, M.E. & Al Mamun, S. 2020. Changes of heavy metal concentrations in Shitalakhya River water of Bangladesh with seasons. *Indonesian Journal of Science and Technology* 5(3): 395-409.

Kuznetsov, A.B., Ovchinnikova, G.V., Semikhatov, M.A., Gorokhov, I.M., Kaurova, O.K., Trupenin, M.T., Vasil'eva, I.M., Gorokhovskii, B.M. & Maslov, A.V. 2008. The Sr isotope characterization and Pb–Pb ages of carbonates rocks from the Satka Formation, the lower Riphean Burzyan Group of the Southern Urals. *Stratigr. Geol. Correl.* 16: 120-137.

Ma, L., Dang, D.H., Wang, W., Evans, R.D. & Wang, W.X. 2019. Rare earth elements in the Pearl River Delta of China: Potential impacts of the REE industry on water, suspended particles and oysters. *Environmental Pollution* 244: 190-201.

Madhavaraju, J., Löser, H., Lee, Y.I., Santacruz, R.L. & Pi-Puig, T. 2016. Geochemistry of lower cretaceous limestones of the Alisitos Formation, Baja California, Mexico: Implications for REE source and paleo-redox conditions. *Journal of South American Earth Sciences* 66: 149-165.

Maryanto, S. 2014. Limestone Microfacies of Baturaja Formation along Air Rambangnia Traverse, South OKU, South Sumatra. *Indonesian Journal on Geoscience* 1(1): 21-34.

Maryanto, S. 2007. Petrografi dan proses diagenesis batugamping Formasi Baturaja di lintasan Air Saka, OKU Selatan, Sumatera Selatan. *Jurnal Sumber Daya Geologi* 17(1): 13-31.

Mir, A.R. 2015. Rare earth element geochemistry of Post-to Neo-archean shales from Singhbhum mobile belt, Eastern India: Implications for tectonic setting and paleo-oxidation conditions. *Chinese Journal of Geochemistry* 34(3): 401-409.

Okuyucu, C., Vachard, D. & Göncüoğlu, M.C. 2013. Refinements in biostratigraphy of the foraminiferal zone MFZ11 (late early Viséan, Mississippian) in the Cebeciköy Limestone (Istanbul Terrane, NW Turkey) and palaeogeographic implications. *Bulletin of Geosciences* 88(3): 621-645.

Palomares, R.M., Hernández, R.L. & Frías, J.M. 2012. Mechanisms of trace metal enrichment in submarine, methane-derived carbonate chimneys from the Gulf of Cadiz. *Journal of Geochemical Exploration* 112: 297-305.

Phewnil, O.A., Tungkananurak, N., Panichsakpatana, S., Pitiyont, B., Siripat, N. & Watanabe, H. 2012. The residues of atrazine herbicide in stream water and stream sediment in Huay Kapo Watershed, Phetchabun Province, Thailand. *Environment and Natural Resources Journal* 10(1): 42-52.

Romero, J.A.S., Lafon, J.M., Nogueira, A.C.R. & Soares, J.L. 2013. Sr isotope geochemistry and Pb–Pb geochronology of the Neoproterozoic cap carbonates, Tangará da Serra, Brazil. *International Geology Review* 55(2): 185-203.

Todd, T.W. 1966. Petrogenetic classification of carbonate rocks. *Journal of Sedimentary Research* 36(2): 317-340.

Usman, U.A., Abdulkadir, A.B., El-Nafaty, J.M., Bukar, M. & Baba, S. 2018. Lithostratigraphy and geochemical characterization of limestone deposits around Kushimaga Area in Yobe of North-Eastern Nigeria. *Nigerian Journal of Technology* 37(4): 885-897.

Veizer, J. 1983. Trace elements and isotopes in sedimentary carbonates. *Reviews in Mineralogy and Geochemistry* 11(1): 265e299.

Vishnevskaya, I.A., Kochnev, B.B., Letnikova, E.F., Kuznetsov, A.B. & Proshenkin, A.I. 2012. Sr isotopic characteristic of neoproterozoic carbonate sediments from the southern Yenisei Ridge. *Doklady Earth Sciences* 443(2): 431-435.

Yousefi, M., Kamkar-Rouhani, A. & Carranza, E.J.M. 2012. Geochemical mineralization probability index (GMPI): A new approach to generate enhanced stream sediment geochemical evidential map for increasing probability of success in mineral potential mapping. *Journal of Geochemical Exploration* 115: 24-35.

Zhang, K.J., Li, Q.H., Yan, L.L., Zeng, L., Lu, L., Zhang, Y.X., Hui, J., Jin, X. & Tang, X.C. 2017. Geochemistry of limestones deposited in various plate tectonic settings. *Earth-Science Reviews* 167: 27-46.

*Corresponding author; email: ronaldoirzon18@gmail.com